Conf-941124--13

PNL-SA-24087

ENHANCING THE DESIGN OF IN SITU CHEMICAL BARRIERS WITH MULTICOMPONENT REACTIVE TRANSPORT MODELING

S. D. Sevougian
C. I. Steefel
S. B. Yabusaki

November 1994

Presented at the
Thirty-Third Hanford Symposium on Health and the Environment Conference
November 7-11, 1994
Richland, Washington

Prepared for
the U.S. Department of Energy
under Contract DE-AC06-76RLO 1830

Pacific Northwest Laboratory
Richland, Washington 99352

DISCLAIMER

DISCLAIMER

Portions of this document may be illegible in electronic image products. Images are produced from the best available original document.

ENHANCING THE DESIGN OF *IN SITU* CHEMICAL BARRIERS WITH MULTICOMPONENT REACTIVE TRANSPORT MODELING

S. David Sevougian, Carl I. Steefel, and Steven B. Yabusaki
Pacific Northwest Laboratory, MSIN K3-61, Richland, WA 99352; (509) 375-4392; FAX: (509) 375-6954

This paper was prepared for presentation at the Thirty-Third Hanford Symposium on Health and the Environment to be held in Pasco, Washington, U.S.A., November 7-11, 1994

Key Words: reactive transport, *in situ* remediation, redox, heterogeneities, chemical kinetics

ABSTRACT

This paper addresses the need for systematic control of field-scale performance in the emplacement and operation of *in situ* chemical treatment barriers; in particular, it addresses the issue of how the local coupling of reaction kinetics and material heterogeneities at the laboratory or bench scale can be accurately upscaled to the field. The authors have recently developed modeling analysis tools that can explicitly account for all relevant chemical reactions that accompany the transport of reagents and contaminants through a chemically and physically heterogeneous subsurface rock or soil matrix. These tools are incorporated into an enhanced design methodology for *in situ* chemical treatment technologies, and the new methodology is demonstrated in the ongoing design of a field experiment for the *In Situ* Redox Manipulation (ISRM) project at the U.S. Department of Energy (DOE) Hanford Site. The ISRM design approach, which systematically integrates bench-scale and site characterization information, provides an ideal test for the new reactive transport techniques. The need for the enhanced chemistry capability is demonstrated by an example that shows how intra-aqueous redox kinetics can affect the transport of reactive solutes. Simulations are carried out on massively parallel computer architectures to resolve the influence of multiscale heterogeneities on multicomponent, multidimensional reactive transport. The technology will soon be available to design larger-scale remediation schemes.

1. INTRODUCTION

Groundwater contaminant plumes that are dispersed over large areas and located hundreds of feet below the ground surface are difficult to treat with excavation or pump-and-treat methods. Therefore, a number of *in situ* treatment technologies have been proposed to address the remediation of these plumes. For example, *in situ* chemical remediation is often based on the creation of a subsurface zone or "barrier" where migrating contaminants will be intercepted and either destroyed or permanently immobilized. The successful design of these permeable chemical barriers requires the ability to engineer two sets of chemical interactions: (1) between the reagent and the local subsurface environment, in order to emplace the barrier; and (2) between the created barrier and the migrating contaminants, in order to effect remediation. These interactions will be different at each contaminated site and, in fact, vary within a given site. Thus, a major and heretofore unaddressed challenge is to design for the systematic control of these chemical reactions under the naturally variable or heterogeneous conditions found in the field.

Standard groundwater transport models being used to design *in situ* barriers simplify the chemistry to an unacceptable degree (e.g., by using only decay and retardation). They cannot adequately account for field-scale performance issues arising from complex chemical reactions in heterogeneous subsurface environments. These issues, which can significantly affect barrier performance, include permeability and flow-field modification by mineral precipitation (Walsh et al., 1982; Hekim et al., 1982; Ortoleva et al., 1987; Novak, 1993; Steefel and Lasaga, 1994; Sevougian et al., 1994), alteration of barrier reactivity arising from mineral dissolution and surface reactions (Stumm and Morgan, 1981; Helgeson et al., 1984; Lichtner, 1985), the propagation of chemical waves (Walsh et al., 1984; Bryant et al., 1987; Dria et al., 1987; Novak et al., 1991; Lichtner, 1992; Novak and Sevougian, 1993; Sevougian et al., 1993), and simultaneous equilibrium and kinetic reactions (Bahr and Rubin, 1987; Brusseau et al., 1989; Yeh and Tripathi, 1991; Friedly, 1991; Steefel and Lasaga, 1992; Sevougian et al., 1993). Inadequate modeling of these phenomena in a heterogeneous aquifer can require expensive overdesign and/or result in an

increased risk of failure.

The new methodology described here is a quantitative approach that attempts to address all of the issues described above. It seeks to systematically control the field-scale performance of *in situ* barriers by coupling a detailed model of local chemical interactions to a realistic model of field-scale physical and chemical heterogeneities. By establishing a more rigorous physical basis, the enhanced methodology effectively uses laboratory and field data, and the resulting barrier designs should be more efficient and reliable.

For example, consider the issue of chemical waves, i.e., traveling variations in the concentration of aqueous species resulting from interaction with mineral phases. These can include both chromatographic waves induced by ion exchange (Rhee et al., 1970; Helfferich and Klein, 1970; Pope et al., 1978; Bryant et al., 1986) or waves resulting from precipitation/dissolution reactions (Schechter et al., 1987; Helfferich, 1989). When a chemical wave breaks through a production well, the concentration of contaminants carried by the wave can increase by many orders of magnitude. Retardation coefficients are often too gross an approximation to accurately predict the time, location, and magnitude of this breakthrough behavior—thus the motivation to couple more detailed reaction mechanisms with solute transport.

The time scale of chemical reactions relative to transport (Jennings and Kirkner, 1984; Schechter, 1991; Lichtner, 1993; Sevougian et al., 1993) is another important issue. Some reactions appear to be fast relative to the rate of fluid flow and can be assumed to be locally in equilibrium; others are slow and must be modeled with a kinetic rate law. This leads to a set of mixed algebraic/differential equations which often requires special numerical methods for their solution (Brenan et al., 1989). Allowing both equilibrium and kinetic reactions in the model increases its flexibility and range of validity, yielding a more accurate design for *in situ* barriers. Below we illustrate the importance of this capability with an example based on the acidification of groundwater near mine tailings.

The methodology described below is flexible enough to address the different combinations of reagents, contaminants, and local geochemistry found at various sites. In particular, we

envision its application to the migration and interaction of a number of contaminants and co-contaminants present at DOE weapons sites. These contaminants include heavy metals, radionuclides, and dissolved organic substances (Riley and Zachara, 1992). For example, at Hanford the contaminants present in the saturated zone include chromium, uranium, and carbon tetrachloride—all of which can be immobilized by permeable *in situ* chemical barriers. In this paper we provide the basic outline and approach of the new design methodology; a future paper will report on the success of the method, once the field results are analyzed.

2. *IN SITU* REDOX MANIPULATION

Although the proposed technology is applicable to any type of permeable *in situ* chemical barrier, we propose to test and prove the enhanced design methodology in support of the *In Situ* Redox Manipulation (ISRM) project sponsored by the Office of Technology Development *In Situ* Remediation Technology Integrated Program. The ISRM project (Fruchter et al., 1993; Amonette et al., 1994; Williams et al., 1994; Gorby and Fruchter, 1994) is in the midst of designing a proof-of-concept field experiment for the emplacement of a chemically reductive barrier. This project employs a systematic design approach that can readily accommodate our recently developed reactive transport modeling tools. We will be able to address all aspects of the ISRM field experiment design using the enhanced design methodology: site characterization, including both physical and chemical heterogeneities; pumping/injection rates and durations; reagent composition, concentration, and stability; monitoring and sampling schemes; and performance indicators.

The ISRM project is designing field experiments to test the feasibility of creating permeable chemical barriers *in situ* by manipulation of the subsurface redox potential. These barriers are zones of reductive redox potential created by interaction of an injected reagent with *in situ* minerals. Specifically, the ISRM project will engineer an abiotic reduction of subsurface materials through reaction with dithionite ion, $S_2O_4^{2-}$. Injection of $S_2O_4^{2-}$ into aquifers containing layered aluminosilicates (clays) has the effect of reducing the structural iron in the clays

from the $Fe^{(III)}$ state to the $Fe^{(II)}$ state. This in turn creates a spatially fixed "chemical barrier" that can intercept and reduce oxidized groundwater contaminants, such as chromium and carbon tetrachloride, thereby significantly lowering their mobility. For example, $Cr^{(VI)}$ is present in much higher concentrations in groundwater than $Cr^{(III)}$. The aqueous concentration of the latter is usually controlled by the solubility of $Cr(OH)_3(s)$, so if the barrier can precipitate this solid, then aqueous Cr is effectively immobilized.

Assuming an iron-rich smectite, the overall reduction of this representative clay by sodium dithionite, $Na_2S_2O_4$, can be written as:

$$2Ca_{0.3}(Fe_2^{(III)}Al_{1.4}Mg_{0.6})Si_8O_{20}(OH)_4 \cdot nH2O + 2Na^+ + S_2O_4^{2-} + 2H_2O$$

$$\Leftrightarrow 2(NaCa_{0.3})(Fe^{(III)}Fe^{(II)}Al_{1.4}Mg_{0.6})Si_8O_{20}(OH)_4 \cdot nH2O + 2SO_3^{2-} + 4H^+ \qquad (1)$$

In this reaction, each electron contributed by dithionite reduces an $Fe^{(III)}$ atom in the clay. The additional –1 charge in the clay structure is shown to be balanced by a concurrent adsorption of interlayer Na^+ ions, although either Ca^{2+} or $FeOH^+$ could also be adsorbed, with the $FeOH^+$ being contributed by dissolution of the iron oxides present in the sediment. For simplicity we have not shown the reduction of structural $Fe^{(III)}$ by dehydroxylation or by semiconductor-like, conductivity-band electrons (Gan et al., 1992). The rate of reaction 1 must be determined experimentally, along with the equilibrium constant for the reaction. Since the rate may be controlled by the amount of $S_2O_4^{2-}$ adsorbed on the clays, it will probably be necessary to include adsorption isotherms or surface complexation data to accurately describe the dissolution process (e.g., Hering and Stumm, 1990).

Other reactions may be important, too. For example, dithionite ion disproportionates to thiosulfate, $S_2O_3^{2-}$, and bisulfite, HSO_3^-, according to the reaction (Cotton and Wilkinson, 1980, p. 535)

$$2S_2O_4^{2-} + H_2O \rightarrow S_2O_3^{2-} + 2HSO_3^- \qquad (2)$$

This disproportionation has a half-life on the order of a day (Amonette et al., 1994), which is

comparable to the time required to emplace the barrier. Also important is the reversible dissociation of $S_2O_4^{2-}$ to the free radical $\dot{S}O_2^-$:

$$S_2O_4^{2-} \Leftrightarrow 2\dot{S}O_2^- \tag{3}$$

It is likely that reduction of $Fe^{(III)}$ in the clay structure is mainly caused by these highly reactive free radicals (Gan et al., 1992; Amonette et al., 1994) rather than by direct reaction with the dithionite ion.

In addition, other reactions may occur in the subsurface that can affect the success of the redox manipulation. The dithionite may react preferentially, for example, with other metal (hydr)oxides in the aquifer, thus limiting the amount of structural iron in the clays that can be reduced. For instance, reduction and dissolution of ferric (hydr)oxides will increase the aqueous concentration of Fe^{2+}, which could in turn precipitate siderite, $FeCO_3(s)$. Other possible precipitates could include calcium sulfites and thiosulfates. Also, as discussed below, intra-aqueous oxidation/reduction reactions can occur, for example, between $O_2(aq)$ and $S_2O_4^{2-}$. The design analysis must be able to account for all of these reactions, some of which may be at equilibrium and some of which may proceed at a finite rate. Furthermore, these reactions must be linked to the transport processes that predominate during the ISRM test. The coupling of the transport processes to the reaction processes is particularly important, since they are likely to occur over a similar time scale of days.

In summary, a whole range of different chemical mechanisms must be modeled to accurately design the redox manipulation test, including precipitation/dissolution, adsorption, ion exchange, oxidation/reduction, intra-aqueous speciation, and surface complexation. The relevant transport processes include advection, diffusion, and dispersion.

3. COUPLING DETAILED CHEMISTRY TO TRANSPORT

Despite the importance, effort, and cost of quantifying reagent chemistry in the subsurface, reactive transport modeling tools have not been generally available to provide a systematic

(physically based) scale-up of understanding at the laboratory scale to barrier performance in the field. Designing the appropriate specification of injection rates, durations, and concentrations to achieve optimal control at the field scale is problematic without explicit consideration of chemical reactions coupled to physical transport processes. Without a systematic understanding of the interacting processes, several field experiments will be necessary to gain knowledge of field-scale barrier performance. Furthermore, these field experiments will have to be repeated each time a new reagent, contaminant, or site is considered. This is an extremely costly approach that will not be feasible for most applications of the *in situ* chemical barrier technology. The result is that most designs will be based on insufficient knowledge and, thus, will not be cost-effective.

To address these important issues, the new design technology includes the following features: (1) the ability to model an arbitrary number and variety of simultaneous chemical processes; (2) the capacity to couple reactions occurring at disparate time scales, i.e., simultaneous equilibrium and kinetic reactions (Sevougian et al., 1993); (3) the capability to correctly combine all of these reactions with fluid transport; (4) the potential to readily incorporate new experimental data as they become available without the need to redesign or reprogram (i.e., to read data as input, rather than by hardcoding); and (5) the option of using several widely accepted chemical databases (Felmy et al., 1984; Wolery, 1992). The reactive transport modeling tools developed by the authors account for all geochemical reactions important to *in situ* remediation technologies: precipitation/dissolution, adsorption, ion exchange, oxidation/reduction, intra-aqueous speciation, and surface speciation. A fundamental feature of these chemistry tools is their portability and adaptability to a wide variety of *in situ* treatments.

4. INTRA-AQUEOUS REDOX KINETICS

For the chemical barrier described above, in which dithionite ion is used to manipulate the *in situ* redox potential, it may be necessary to explicitly incorporate intra-aqueous redox kinetics in the modeling tools. The importance of redox kinetics in natural waters has received significant

attention in the literature (e.g., Jackson and Patterson, 1982; Barcelona and Naymik, 1984; Lindberg and Runnels, 1984; van Beek and van Puffelen, 1987; Rose and Long, 1988; Barcelona et al., 1989; Eary and Schramke, 1990), but much research remains to be done regarding its effect on reactive solute transport in chemically and physically heterogeneous aquifers (Liu and Narasimhan, 1989a,b; Postma et al., 1991). Until now, most reaction-transport analyses have assumed overall redox equilibrium (indeed, many existing models still assume equilibrium for all reactions), neglecting important differences in the half-lives of various redox couples. For example, at low pH the oxidation kinetics of several elements, such as arsenic and iron, can be very slow. These rate limitations may have a significant effect on the propagation of reactive contaminant plumes.

Recently, we investigated the influence of intra-aqueous redox kinetics on the movement of reactive contaminants and found that intra-aqueous iron redox kinetics can have a significant effect during the oxidation of pyrite, with spatial disequilibrium ranging from the millimeter to the tens-of-meters scale, depending on the reactive surface area. It is likely that this effect could be significant in the abiotic reduction of clays by dithionite and subsequent reduction of contaminants in the ISRM project (see Eq. 1), particularly because it has been established that the dithionite ion itself is unstable in aqueous solution (Eqs. 2 and 3). Thus, it would seem to be advantageous to use more comprehensive reaction software, such as that discussed here, which can model these kinetically controlled intra-aqueous reactions.

Our first effort to quantify the effect of intra-aqueous redox kinetics on contaminant transport has involved the study of acid mine drainage (Sevougian and Steefel, 1993). Drainage water from mine tailings composed of heavy metals such as lead, zinc, and copper usually becomes acidified through the oxidation of pyrite, $FeS_2(s)$, unless it is buffered by carbonate minerals (Stumm and Morgan, 1981). This acidification creates a favorable environment for further leaching of these and other poisonous metals, such as arsenic and molybdenum. The main questions we address in this regard are how important are intra-aqueous redox kinetics, and whether equilibrium reaction modeling suffices to accurately predict metal transport. The scenario

is oxygenated water flowing into a pyritic aquifer or tailings pile, dissolving pyrite to produce ferrous ion, Fe^{2+}, which subsequently may be oxidized to ferric ion, Fe^{3+}. The question is what influence the rate of this intra-aqueous reaction has on the overall redox state of the groundwater, throughout the spatial domain of interest.

There are two important oxidation reactions that dissolve pyrite in mine tailings, one involving $O_2(aq)$ and the other involving Fe^{3+} (McKibben and Barnes, 1986; Moses et al., 1987; Moses and Herman, 1991; Rimstidt and Newcomb, 1993):

$$FeS_2(s) + \frac{7}{2}O_2(aq) + H_2O \rightarrow Fe^{2+} + 2\,SO_4^{2-} + 2\,H^+ \tag{4}$$

$$FeS_2(s) + 14\,Fe^{3+} + 8\,H_2O \rightarrow 15\,Fe^{2+} + 2\,SO_4^{2-} + 16\,H^+ \tag{5}$$

Although both of these oxidation reactions acidify the groundwater through production of H^+ ions, the pyrite-Fe^{3+} reaction (Eq. 5) produces eight times as much H^+ per mole of pyrite dissolved. Thus, if this reaction is able to proceed, the groundwater will acidify much more rapidly. However, the oxidation of Fe^{2+} to Fe^{3+}

$$Fe^{2+} + H^+ + \frac{1}{4}O_2(aq) \rightarrow Fe^{3+} + \frac{1}{2}H_2O \tag{6}$$

is an intermediate reaction between reactions 4 and 5 and can slow the acidification process. If reaction 6 is slow, then little Fe^{3+} is available for reaction 5, whereas if reaction 6 is fast (equilibrium), then the extent of reaction 5 can go much further toward the products, increasing the acidification. A schematic of the pyrite oxidation process is shown in Figure 1.

The relative strengths of $O_2(aq)$ and Fe^{3+} as oxidants of sulfide are shown in the "redox ladder" of Figure 2 (Scott and Morgan, 1990). In this figure, the Fe^{3+} state is depicted as $Fe(OH)_2^+$, since this is the dominant Fe^{3+} species in the pH range considered here. In this redox ladder, the oxidant of a redox couple is on the left side while the reductant is on the right. Furthermore, the strongest oxidants are at the top and the strongest reductants at the bottom of the ladder. Any oxidant of a redox couple can oxidize a reductant that stands on a lower point of the ladder. Thus, we see that HS^- (and also pyrite, which is not shown) would be oxidized first by $O_2(aq)$, and then by Fe^{3+}, if these reactions were equilibrium reactions. In a system with fluid

transport, this reduction sequence will be manifest over space, as well as time, as shown in Figure 3. However, kinetic constraints often modify these equilibrium tendencies, as demonstrated below.

Another important contributor to the acidification process is precipitation of amorphous ferric hydroxide, $Fe(OH)_3(am)$:

$$Fe^{3+} + 3\,H_2O \rightarrow Fe(OH)_3(am) + 3\,H^+ \qquad (7)$$

This reaction also requires a supply of Fe^{3+} ion, so that the intra-aqueous conversion of Fe^{2+} to Fe^{3+} takes on added importance.

To quantify these effects, a one-dimensional reaction-transport example will be shown in which oxygenated water infiltrates a tailings pile containing 4% by volume of $FeS_2(s)$. This example was solved using the geochemical simulator KGEOFLOW (Sevougian, et al., 1994). It solves the advection/dispersion equation in a one-dimensional Eulerian reference frame with any combination of kinetic and equilibrium reactions and any number of chemical species and elements. The elements, aqueous species, and mineral phases used for this example are listed in Table 1. For this example, all intra-aqueous reactions were considered to be at equilibrium, with the exception of Fe reactions. For intra-aqueous Fe reactions we consider two limiting cases: (1) complete intra-aqueous Fe equilibrium, which implies a single Eh for the whole system; and (2) complete intra-aqueous Fe *dis*equilibrium, which implies that the Fe^{3+}–Fe^{2+} Eh is different from the Eh of other redox pairs, such as SO_4^{2-}–HS^- and $O_2(aq)$–H_2O. In this disequilibrium case, all intra-aqueous species composed of Fe^{2+} can react only with each other and not with Fe^{3+}–bearing species.

The steady-state rate profiles, $O_2(aq)$ concentrations, and pH are shown in Figures 3–5, respectively, for these two limiting cases of equilibrium and disequilibrium (after an infiltration period of 20 years). The rate constants and intrinsic rate laws for the two pyrite dissolution reactions are given by (McKibben and Barnes, 1986)

$$r_{FeS_2 + O_{2(aq)}} = 10^{-11.5}\,[O_{2(aq)}]^{0.5} \quad [=] \frac{\text{moles}}{\text{cm}^2 \bullet \text{sec}} \qquad (8)$$

$$r_{FeS_2 + Fe^{3+}} = 10^{-11.5} \frac{\left[\Sigma Fe^{3+}\right]^{0.5}}{[H^+]^{0.5}} \quad [=] \quad \frac{\text{moles}}{\text{cm}^2 \bullet \text{sec}} \tag{9}$$

(McKibben and Barnes (1986) incorrectly reported their pyrite-O_2(aq) rate constant as $10^{-8.5}$; by re-analyzing their concentration vs. time plots we determined the correct value to be that given in Eq. 8.)

Figure 3 illustrates the expected dissolution of pyrite by both Fe^{3+} and O_2(aq) in the intra-aqueous Fe equilibrium case, with Fe^{3+}–FeS_2 oxidation proceeding at a relatively high rate. This results in a rapid decline with distance of both pH and O_2(aq), as shown in Figures 4 and 5. The redox ladder concept, discussed above, is born out for this equilibrium example. Specifically, Figure 3 shows that the O_2(aq) in the infiltrating water is depleted first, i.e., upstream of the depletion of Fe^{3+}. In contrast, for intra-aqueous *dis*equilibrium (Figure 3), only the pyrite-O_2(aq) reaction is possible (since no aqueous Fe^{3+} is produced), but it proceeds at a rate ten times less than the pyrite-Fe^{3+} rate in the equilibrium case. Thus, the decline in pH and O_2(aq) occurs over a much longer distance (Figures 4 and 5). In this example, we have used a pyrite specific surface area of 0.025 cm^2/g, to show the effect of intra-aqueous disequilibrium at a large length scale. At larger values of the surface area, the disparity between intra-aqueous equilibrium and disequilibrium still exists, but will be manifested over a smaller length scale. (Also, although not shown, for the case of intra-aqueous Fe equilibrium, significant precipitation of $Fe(OH)_3$(am) is predicted by the model.)

The above analysis has shown the pH and O_2(aq) behavior for the two extremes of intra-aqueous equilibrium and disequilibrium for reaction 6. The final part of this example is to show where between these two limits experimentally reported rates fall. For this we used an Fe^{2+}–Fe^{3+} rate (Eq. 6) taken from a summary paper of intra-aqueous redox kinetics (Eary and Schramke, 1990):

$$r_{Fe^{2+} \rightarrow Fe^{3+}} = 10^{-5.9} \left[\Sigma Fe^{2+}\right][O_{2(aq)}] \quad [=] \quad \frac{\text{moles}}{\text{liter} \bullet \text{sec}} \tag{10}$$

The results of using Eq. 10 for the intra-aqueous iron reaction are shown in Figures 6 and 7. The

pH and O_2(aq) curves based on the experimentally reported redox kinetics are nearly indistinguishable from those based on complete redox disequilibrium, so it is clear that in this example a geochemical computer model that assumes overall redox equilibrium would be insufficient and inaccurate.

Finally, we wish to ask how much would the intra-aqueous rate have to be changed for the pH and O_2(aq) profiles to go from disequilibrium to equilibrium. This is demonstrated in Figure 8, which shows the O_2(aq) profiles that result when the Fe^{2+}–Fe^{3+} rate is increased by factors of ten (from an initial value labeled as k_o and taken from Eq. 10). It takes an increase of about 100 to show much change from disequilibrium, and an increase of about 1000 to approach the equilibrium result.

In the above analysis we have modeled mineral dissolution as occurring simultaneously by two parallel reaction mechanisms (reactions 4 and 5). This is a new and important feature of the enhanced design methodology, particularly since such reactions are common (Boudart, 1968), especially in redox systems. This capability is not present in a number of other geochemical kinetic codes (e.g., Yeh and Iskra, 1994; Steefel and Lasaga, 1994).

In summary, this example has shown the significant influence that intra-aqueous redox kinetics can have on the degree of spatial disequilibrium and chemical zoning. Although we have specifically dealt with pyrite dissolution, the same effects could easily be observed with reinfiltration of oxygenated water into an *in situ* chemical barrier. Thus it is important to have the capability to model this process during the design of the *in situ* barrier.

5. CHEMICAL AND PHYSICAL HETEROGENEITIES

Laboratory studies provide much of the understanding on which *in situ* treatment technologies are based, yet many field-scale issues simply cannot be addressed in the laboratory. One important issue is the presence of multiple-length-scale physical and chemical heterogeneities, which lead to time-dependent retardation of reactive contaminants that is significantly different from the behavior observed in homogeneous aquifers (Roberts et al., 1986; Kabala and Sposito,

1991; Tompson, 1993).

In this regard, one of the most important influences on the large-scale retardation and breakthrough behavior of contaminants is the degree of spatial correlation between the chemical properties (such as reactive surface area and mineral volume fraction) and the hydraulic conductivity. A negative correlation (usually expected) will yield a much different shape and velocity for the contaminant plume than a positive correlation. Through its effect on the "local" precipitation/dissolution rate, the variability in reactive surface area coupled to the variability in "local" conductivity (i.e., the local correlation) produces differing degrees of reaction front sharpness at various points in the medium. These local reaction fronts interact in a complicated fashion to produce a large-scale or global displacement pattern, which may or may not be accurately duplicated by simple scale-averaging of the chemical and physical properties. A specific example of chemical heterogeneity in the ISRM project is the correlation of clay and iron-(hydr)oxide content and surface area with the local permeability and porosity. This correlation may be the single most important factor determining the success of the reductive barrier. Other important chemical heterogeneities at the ISRM site include the spatial variability of the ion-exchange capacity and the spatial variability of any relevant adsorption K_ds and/or adsorption rate constants.

In summary, the knowledge gap between bench-scale testing and field-scale performance significantly increases the difficulty of designing an effective *in situ* chemical barrier, i.e., one that maintains control over the desired chemical reactions as reagents and contaminants are transported through physically and chemically heterogeneous aquifer materials. The surface-area/conductivity correlation and the heterogeneity distribution at the ISRM experimental site are still under investigation and, when quantified, will represent one of the most important inputs to the new design methodology.

6. ENHANCED DESIGN METHODOLOGY

Based on the above discussions of the importance of modeling detailed chemical mechanisms coupled to transport and the importance of including the effects of both physical and chemical heterogeneity, we present in this section a concise outline of the enhanced design methodology that includes both of these effects. As mentioned earlier, the most important analysis tool in the design methodology is the multidimensional reactive transport code. This code, which is still being actively developed and improved, includes two important features. First is a multicomponent geochemical reaction module that models more of the detailed chemical kinetic mechanisms in subsurface systems than other currently available codes do. This includes all of the reaction mechanisms mentioned earlier, plus the features listed in Section 3, including the capability to model stoichiometrically dependent sets of reactions (parallel reactions). This is a modular program that may be coupled to a variety of state-of-the-art transport codes (e.g., Wheeler et al., 1992) by operator-splitting.

The second important feature is implementation of the multidimensional, coupled, reactive transport model on massively parallel computer architectures. Given the current state of computer technology, it is only with massively parallel architectures that fine-scale and large-scale heterogeneities can be simultaneously simulated for chemically complex, multidimensional systems. Given the naturally occurring physical and chemical heterogeneities at the Hanford Site, the dithionite chemical barrier experiment is an ideal test problem for proving the capabilities of the parallel computer code.

A general methodology for the successful design of *in situ* chemical barriers is given below and illustrated by the flow chart in Figure 9. [Steps 1–3 are not entirely sequential; portions of them may be conducted simultaneously.]

(1) Perform site-characterization studies to analyze subsurface physical and chemical heterogeneities at the proposed field site.

(2) Conduct laboratory studies to measure relevant physical and chemical parameters,

including the "major" rock types at the specific field site. The studies may include batch, bench-scale, and intermediate-scale experiments. Column experiments should be performed on individual sediment or rock types to assess the degree of chemical heterogeneity at the field site, i.e., how many different rock types are necessary to represent the field-scale heterogeneities.

(3) Demonstrate that the software package can describe reactive transport through *individual* sediment types found at the field site, i.e., it can model the local coupling of chemistry and transport.

(4) Optimize the design of the field test with the reactive transport model, based on the combined results of the site-characterization study and the laboratory experiments, taking into account the naturally occurring physical and chemical heterogeneities at the field scale.

(5) Carry out the field or pilot test to create the *in situ* permeable barrier.

(6) Analyze the results of the pilot test to determine the effectiveness of the original design. Use monitoring data to evaluate emplacement success and identify mechanisms causing any deficiencies. Decide on the final design for full-scale aquifer remediation.

Since steps 3, 4, and 6 are the primary focus of the enhancement outlined in this paper, let us amplify them:

Step 3: In this step the reaction-transport analysis is restricted to one-dimensional flow in a homogeneous medium (i.e., a column) through a number of sediment types representative of the field site, each of which is chemically and physically homogeneous. This primarily involves extraction of the important chemical parameters (solubilities, sorption constants, rate constants, etc.) from the batch and column studies and incorporation of these data into the design analysis.

Step 4: This step integrates the information from the individual column experiments that were analyzed in step 3 with data from the site characterization studies, in order to provide a design capable of describing reactive transport through the physically and chemically heterogeneous test site. That is, by systematic averaging or upscaling of the properties of the individual sediment types to the field scale, flow and reactive transport behavior at the field scale can be predicted. This will depend on both accurate chemical analysis of all the pertinent sediment types and accurate

characterization of their distribution in the aquifer. The most important analysis tool for this step is the 3-D reactive transport model.

One of the principal roles of step 4 is an analysis of the sensitivity of the design to various physical and chemical parameters. This consists of systematically testing the sensitivity of the expected results to physical parameters (such as the permeability and porosity distribution) and to chemical parameters (such as the distribution of reactive phases determined in the site characterization studies). This analysis is important because it is likely that uncertainties in the distribution of reactive phases and their correlation with permeability may still exist after the site characterization. With a sensitivity analysis, it is possible to determine whether the uncertainties in the site characterization (which should be quantifiable) are likely to affect the success of the *in situ* permeable barrier. It is also possible to test the sensitivity of the system to various pumping rates and to the concentrations of the reagents used in the remediation. The sensitivity analysis will be used to optimize the design of several aspects of the remediation technology: (a) the formation of the original permeable chemical barrier (in the case of the ISRM experiment, this is the reduction of structural iron in clays by dithionite injection); (b) the longevity of the chemical barrier (in this segment, the software package is used to describe the physical and chemical processes over time that may act to destroy the chemical barrier; in the case of the ISRM experiment, this involves primarily the re-infiltration of oxygen into the remediation site and subsequent re-oxidation of structural iron in the clays); and (c) performance assessment of the barrier for the actual contaminant(s) of interest (in the case of the ISRM experiment, this analysis would involve the chemical migration of chromium). The sensitivity analyses will emphasize those processes and parameters that are likely to most significantly impact the efficiency and success of the ultimate remediation process.

Step 6: This step consists of the post-test interpretation of the monitoring data. Most importantly, the interpretation will use the same reactive transport model as was used in the original design and sensitivity analysis of the field test. The use of a consistent approach is essential for the efficient design of remediation strategies, since it allows the engineer to systematically improve the

performance of the pilot test and the final remediation technology. Formulated in this way, the interpretation of the field data becomes part of an iterative process in which the parameters and processes identified in steps 3 and 4 will be evaluated and adjusted where appropriate to reflect the new understanding of the processes involved.

The post-test interpretation will focus on (a) the overall efficiency of the barrier emplacement and the factors that determine that efficiency, and (b) the issue of natural physical and chemical heterogeneities that may have affected the results. For example, in the ISRM experiment, the correlations between reactive site distributions and permeability in the porous matrix at the field site are likely to have a very important effect on the efficiency of the barrier emplacement. The field test, in conjunction with the post-test interpretation, provide essential information that can be used to improve subsequent designs. The issues addressed in the original design of the field test, including (a) formation of the barrier, (b) longevity of the barrier, and (c) performance assessment of the barrier with an actual contaminant, will also be addressed in the post-test interpretation.

Without a comprehensive design methodology that accounts for chemical reactions coupled to transport, one may have to iterate between steps 5 and 6 a number of times to reach an optimum. This iteration process could be very expensive. However, with the ability of the reactive transport modeling tools to check design sensitivity against system parameters, the number of iterations can be reduced greatly or eliminated altogether. The success of this depends on modeling all the important chemical processes with the correct coupling to fluid transport in a heterogeneous aquifer. The chemical heterogeneity column experiments are essential to this step. Also, the ability to optimize the barrier emplacement design in a timely fashion is contingent on the ability to specify user input at run-time instead of engaging in costly reprogramming.

Testing the above step-by-step design at the ISRM site will demonstrate the benefit of the new methodology for one particular remediation at one particular site. Depending on the success of the experiment, the next logical step is to design a larger-scale *in situ* barrier at a different site or over a larger area that may encompass the original test site. A site characterization study would still be required at a new site to identify the distribution of physical and chemical properties. However,

based on the experience gained in the pilot test and the ability of the new software tools to test many different scenarios (e.g., various compositions of the injected solution and various pumping rates), the laboratory effort should be reduced.

7. CONCLUSIONS

By explicitly including chemical reactions and chemical heterogeneity in the field-scale transport analyses, the enhanced design methodology will result in more efficient and reliable barrier emplacement and performance. The enhanced methodology is flexible and readily adaptable to all subsurface permeable chemical barrier technologies. Therefore it will be applicable not only to groundwater restoration at DOE sites, but also to Department of Defense and industrial sites. It has applicability to a wide variety of contaminants, including heavy metals, radionuclides, and dissolved organics.

Some of the more important direct benefits will include (1) more optimal design of *in situ* permeable barriers, resulting in greater effectiveness in trapping contaminants; (2) greater efficiency and speed in designing new barriers; (3) enhanced ability to anticipate potential problems, thereby reducing the risk of failure; (4) improved assessment of the barrier performance and longevity; (5) enhanced value of existing physical and chemical data; (6) improved design of required laboratory experiments; (7) increased efficiency in testing the sensitivity of the treatment to various physical parameters; and (8) greater ease of including new information in the design.

A key point is the anticipated reduction in the number of laboratory and field experiments, which can significantly decrease the design cost. In particular, after the initial laboratory and site-characterization studies to calibrate the reactive transport model, design modifications and optimization of the *in situ* treatment require fewer laboratory and pilot tests than if these tools were not available. The importance of modeling detailed reaction mechanisms, including parallel dissolution schemes for the same mineral, is demonstrated through an example based on intra-aqueous redox kinetics.

ACKNOWLEDGMENT

Work was supported by funds from the Environmental and Molecular Sciences Laboratory Construction Project at Pacific Northwest Laboratory. Pacific Northwest Laboratory is operated for the U. S. Department of Energy by Battelle Memorial Institute under Contract DE-AC06-76RLO 1830.

REFERENCES

Amonette, J. E., J. E. Szecsody, J. C. Templeton, Y. A. Gorby, and J. S. Fruchter. 1994. Abiotic reduction of aquifer materials by dithionite: The promise for *in situ* remediation. In: *In-Situ Remediation: Scientific Basis for Current and Future Technologies*, proceedings of the 33rd Hanford Symposium on Health and the Environment. Pasco, WA.

Bahr, J. M., and J. Rubin. 1987. Direct comparison of kinetic and local equilibrium formulations for solute transport affected by surface reactions. *Water Resour. Res.* 23:438-452.

Barcelona, M. J. and T. G. Naymik. 1984. Dynamics of a fertilizer contaminant plume in groundwater. *Environ. Sci. Technol.* 18:257–261.

Barcelona, M. J., T. R. Holm, M. R. Schock, and G. K. George. 1989. Spatial and temporal gradients in aquifer oxidation-reduction conditions. *Water Resour. Res.* 25:991–1003.

Boudart, M. 1968. *Kinetics of Chemical Processes.* Prentice-Hall, Englewood Cliffs, New Jersey.

Brenan, K. E., S. L. Campbell, and L. R. Petzold. 1989. *Numerical Solution of Initial-Value Problems in Differential-Algebraic Equations.* Elsevier, New York.

Brusseau, M. L., R. E. Jessup, and P. S. C. Rao. 1989. Modeling the transport of solutes influenced by multiprocess nonequilibrium. *Water Resour. Res.* 25:1971–1988.

Bryant, S. L., R. S. Schechter, and L. W. Lake. 1986. Interactions of precipitation/dissolution waves and ion exchange in flow through permeable media. *AIChE J.* 32:751–764.

Bryant, S. L., R. S. Schechter, and L. W. Lake. 1987. Mineral sequences in precipitation/dissolution waves. *AIChE J.* 33:1271–1287.

Cotton, F. A. and G. Wilkinson. 1980. *Advanced Inorganic Chemistry, Fourth Edition.* John Wiley & Sons, Inc., New York.

Dria, M. A., S. L. Bryant, R. S. Schechter, and L.W. Lake. 1987. Interacting precipitation/dissolution waves: the movement of inorganic contaminants in groundwater. *Water Resour. Res.* 23:2076–2090.

Eary, L. E. and J. A. Schramke. 1990. Rates of Inorganic Oxidation Reactions Involving Dissolved Oxygen. In: *Chemical Modeling of Aqueous Systems II*, pp. 379–396, D. C. Melchior and R. L. Bassett (eds.). American Chemical Society, Washington, D.C.

Felmy, A. R., D. C. Girvin, and E. A. Jenne. 1984. *MINTEQ—A Computer Program for Calculating Aqueous Geochemical Equilibria,* US EPA Rep. 600/3-84-032. Natl. Tech. Inf. Serv., Springfield, VA 22161.

Friedly, J. C. 1991. Extent of reaction in open systems with multiple heterogeneous reactions. *AIChE. J.* 37:687–693.

Fruchter, J. S., F. A. Spane, J. K. Fredrickson, C. R. Cole, J. E. Amonette, J. C. Templeton, T. O. Stevens, D. J. Holford, L. E. Eary, J. M. Zachara, B. N. Bjornstad, G. D. Black, and V. R. Vermeul. 1993. Manipulation of Natural Subsurface Processes: Field Research and Validation. In: *Pacific Northwest Laboratory Annual Report for 1992 to the DOE Office of Energy Research, Part 2: Environmental Sciences.* p. 127. PNL-8500 Pt. 2/UC-407, Pacific Northwest Laboratory, Richland, WA 99352.

Gan, H., J. W. Stucki, and G. W. Bailey. 1992. Reduction of structural iron in ferruginous smectites by free radicals. *Clays Clay Miner.* 40:659–665.

Gorby, Y. A., and J. S. Fruchter. 1994. *In situ* remediation of contaminated subsurfaces by metal-reducing bacteria. In: *In-Situ Remediation: Scientific Basis for Current and Future Technologies*, proceedings of the 33rd Hanford Symposium on Health and the Environment. Pasco, WA.

Hekim, Y., H. S. Fogler, and C. C. McCune. 1982. The radial movement of permeability fronts and multiple reaction zones in porous media. *SPEJ.* (Feb.):99–107.

Helfferich, F. G. 1989. The theory of precipitation/dissolution waves. *AIChE J.* 35:75–87.

Helfferich, F. G., and G. Klein. 1970. *Multicomponent Chromatography.* Marcel Dekker, New York.

Helgeson, H. C., W. M. Murphy, and P. Aagaard. 1984. Thermodynamic and kinetic constraints on reaction rates among minerals and aqueous solutions. II. Rate constants, effective surface area, and the hydrolysis of feldspar. *Geochim. Cosmochim. Acta.* 48:2405-2432.

Hering, J. G. and W. Stumm. 1990. Oxidative and Reductive Dissolution of Minerals. In: *Mineral-Water Interface Geochemistry*, pp. 427–459, M. F. Hochella and A. F. White (eds.). *Reviews in Mineralogy, Vol. 23*, Mineralogical Society of America, Washington, D.C.

Jackson, R. E. and R. J. Patterson. 1982. Interpretation of pH and Eh trends in a fluvial-sand aquifer system. *Water Resour. Res.* 18:1255-1268.

Jennings, A. A. and D. J. Kirkner. 1984. Instantaneous equilibrium approximation analysis. *J. Hydraulic Eng.* 110:1700–1717.

Kabala, Z. J. and G. Sposito. 1991. A stochastic model of reactive solute transport with time-varying velocity in a heterogeneous aquifer. *Water Resour. Res.* 27:341-350.

Lichtner, P. C. 1985. Continuum model for simultaneous chemical reactions and mass transport in hydrothermal systems. *Geochim. Cosmochim. Acta.* 49:779–800.

Lichtner, P. C. 1992. Time-space continuum description of fluid/rock interaction in permeable media. *Water Resour. Res.* 28:3135–3155.

Lichtner, P. C. 1993. Scaling properties of time-space kinetic mass transport equations and the local equilibrium limit. *Am. J. Sci.* 293:257–296.

Lindberg, R. D. and D. D. Runnells. 1984. Ground water redox reactions: An analysis of equilibrium state applied to Eh measurements and geochemical modeling. *Science*. 225:925-927.

Liu, C. W. and T. N. Narasimhan. 1989a. Redox-controlled multiple-species reactive chemical transport, 1. Model development. *Water Resour. Res.* 25:869-882.

Liu, C. W. and T. N. Narasimhan. 1989b. Redox-controlled multiple-species reactive chemical transport, 2. Verification and application. *Water Resour. Res.* 25:883-910.

McKibben, M. A. and H. L. Barnes. 1986. Oxidation of pyrite in low temperature acidic solutions: Rate laws and surface textures. *Geochim. Cosmochim. Acta.* 50:1509–1520.

Moses, C. O. and J. S. Herman. 1991. Pyrite oxidation at circumneutral pH. *Geochim. Cosmochim. Acta.* 55:471–482.

Moses, C. O., K. Nordstrom, J. S. Herman, and A. L. Mills. 1987. Aqueous pyrite oxidation by dissolved oxygen and by ferric iron. *Geochim. Cosmochim. Acta.* 51:1561–1571.

Novak, C. F. 1993. Modeling mineral dissolution and precipitation in dual-porosity fracture-matrix systems. *J. Contam. Hydrol.* 13:91–115.

Novak, C. F. and S. D. Sevougian. 1993. Propagation of Dissolution/Precipitation Waves in Porous Media. In: *Migration and Fate of Pollutants in Soils and Subsoils*, pp. 275–307. NATO ASI Series, Series G: Ecological Sciences, Vol. 32, D. Petruzzelli and F. G. Helfferich (eds.). Springer-Verlag, Berlin, Germany.

Novak, C. F., L. W. Lake, and R. S. Schechter. 1991. Geochemical modeling of two-phase flow with interphase mass transfer. *AIChE J.* 37:1625–1633.

Ortoleva, P., E. Merino, C. Moore, and J. Chadam. 1987. Geochemical self-organization I: Reaction-transport feedbacks and modeling approach. *Am. J. Sci.* 287:979–1007.

Postma, D., C. Boesen, H. Kristiansen, and F. Larsen. 1991. Nitrate reduction in an unconfined sandy aquifer: water chemistry, reduction processes, and geochemical modeling. *Water Resour. Res.* 27:2027–2045.

Pope, G. A., L. W. Lake, and F. G. Helfferich. 1978. Cation exchange in chemical flooding: Part 1—Basic theory without dispersion. *SPEJ.* (Dec.):418–434.

Rhee, H. K., R. Aris, and N. R. Amundson. 1970. Theory of multicomponent chromatography. *Philos. Trans. R. Soc. London.* A267:419–455.

Riley, R. G. and J. M. Zachara. 1992. *Chemical Contaminants on DOE Lands and Selection of Contaminant Mixtures for Subsurface Science Research.* U.S. DOE Report No. DOE/ER-0547T. Natl. Tech. Inf. Serv., Springfield, VA 22161.

Rimstidt, J. D. and W. D. Newcomb. 1993. Measurement and analysis of rate data: The rate of reaction of ferric iron with pyrite. *Geochim. Cosmochim. Acta.* 57:1919–1934.

Roberts, P. V., M. N. Goltz, and D. M. Mackay. 1986. A natural gradient experiment on solute transport in a sand aquifer: 3. Retardation estimates and mass balances for organic solutes. *Water Resour. Res.* 22:2047–2058.

Rose, S. and A. Long. 1988. Dissolved oxygen systematics in the Tuscon Basin aquifer. *Water Resour. Res.* 24:127-136.

Schechter, R. S. 1991. *Oil Well Stimulation.* Prentice-Hall, Englewood Cliffs, N.J.

Schechter, R. S., S. L. Bryant, and L. W. Lake. 1987. Isotherm–free chromatography: propagation of precipitation/dissolution waves. *Chem. Eng. Comm.* 58:353–376.

Scott, M. J. and J. J. Morgan. 1990. Energetics and Conservative Properties of Redox Systems. In: *Chemical Modeling of Aqueous Systems II*, pp. 368–378, D. C. Melchior and R. L. Bassett (eds.). American Chemical Society, Washington, D.C.

Sevougian, S. D. and C. I. Steefel. 1993. Effect of redox disequilibrium on reactive solute transport in chemically heterogeneous aquifers. *Eos, Transactions, Am. Geophys. Union.* 74(43):281.

Sevougian, S. D., R. S. Schechter, and L. W. Lake. 1993. Effect of partial local equilibrium on the propagation of precipitation/dissolution waves. *Ind. Eng. Chem. Res.* 32(10):2281–2304.

Sevougian, S. D., L. W. Lake, and R. S. Schechter. 1994. A new geochemical simulator to design more effective sandstone acidizing treatments, SPE 24780, presented at the 67th Annual Technical Conference and Exhibition of the Society of Petroleum Engineers, Washington, D.C., Oct. 4-7, 1992, accepted for publication in *SPE Prod. & Facil.*, 1994.

Steefel, C. I. and A. C. Lasaga. 1992. Putting transport into water-rock interaction models. *Geology.* 20:680–684.

Steefel, C. I. and A. C. Lasaga. 1994. A coupled model for transport of multiple chemical species and kinetic precipitation/dissolution reactions with application to reactive flow in single phase hydrothermal systems. *Am. J. Sci.* 294:529–592.

Stumm, W. and J. J. Morgan. 1981. *Aquatic Chemistry.* John Wiley & Sons, Inc., New York.

Tompson, A. F. B. 1993. Numerical simulation of chemical migration in physically and chemically heterogeneous porous media. *Water Resour. Res.* 29:3709–3726.

van Beek, C. G. E. M. and J. van Puffelen. 1987. Changes in the chemical composition of drinking water after well infiltration in an unconsolidated sandy aquifer. *Water Resour. Res.* 23:69-76.

Walsh, M. P., L. W. Lake, and R. S. Schechter. 1982. A description of chemical precipitation mechanisms and their role in formation damage during stimulation by hydrofluoric acid. *J. Pet. Tech.* 34:2097–2112.

Walsh, M. P., S. L. Bryant, R. S. Schechter, and L. W. Lake. 1984. Precipitation and dissolution of solids attending flow through porous media. *AIChE J.* 30:317–328.

Wheeler, M. F., K. R. Roberson, and Ashokkumar Chilakapati. 1992. Three-Dimensional Bioremediation Modeling in Heterogeneous Porous Media. In: *Vol II: Numerical Methods in Water Resources*, T. F. Russell et al. (eds.). Computational Mechanics Publications, Southhampton, UK.

Williams, M. D., S. B. Yabusaki, and C. R. Cole. 1994. *In situ* manipulation field experiment: design analysis. In: *In-Situ Remediation: Scientific Basis for Current and Future Technologies*, proceedings of the 33rd Hanford Symposium on Health and the Environment. Pasco, WA.

Wolery T. J. 1992. *EQ3NR, A Computer Program for Geochemical Aqueous Speciation-Solubility Calculations: Theoretical Manual, User's Guide, and Related Documentation, Version 7.0*, Publ UCRL-MA-110662 PT III. Lawrence Livermore National Laboratory, Livermore, CA, 94551.

Yeh, G. T. and V. S. Tripathi. 1989. A critical evaluation of recent developments in hydrogeochemical transport models of reactive multichemical components. *Water Resour. Res.* 25:93–108.

Table 1—Elements, minerals, and aqueous species used in pyrite oxidation simulations.

Elements	Minerals	Aqueous Species	
Hydrogen	FeS_2 (pyrite)	H_2O	HS^-
Oxygen	$Fe(OH)_3$(am)	H^+	H_2
Iron	FeOOH (goethite)	Cl^-	Fe^{3+}
Sulfur	FeS (pyrrhotite)	Fe^{2+}	$Fe(OH)_3$
Chlorine	S (sulfur)	SO_4^{2-}	$Fe(OH)_2$
	$Fe(OH)_2$	$Fe(OH)_2^+$	$Fe(SO_4)_2^-$
	$FeSO_4$	$FeSO_4$	$Fe(OH)_4^-$
		HSO_4^-	S^{2-}
		H_2S	HO_2^-
		OH^-	O_2
		H_2SO_4	

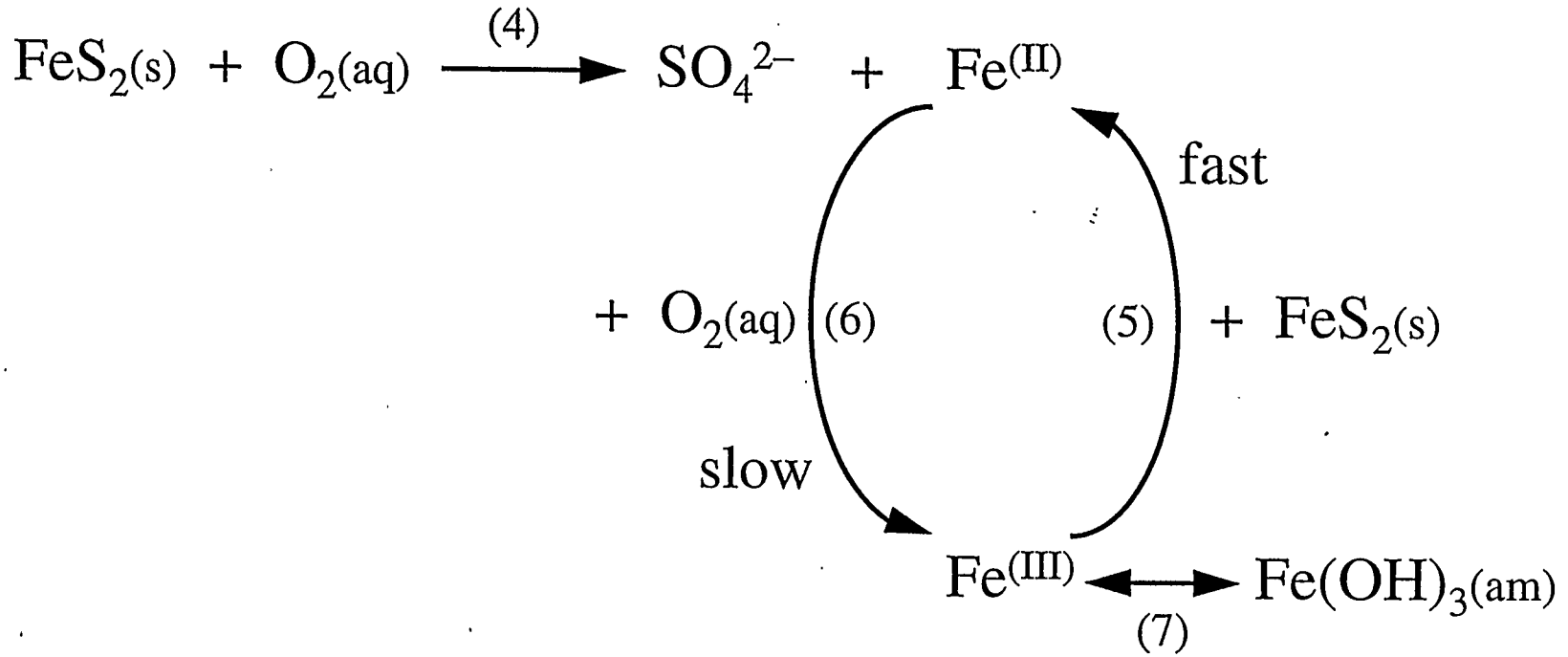
FeS2(s) + O2(aq)
(4)
SO4 2–
+ Fe(II)
fast
+ O2(aq)
(6)
(5)
+ FeS2(s)
slow
Fe(III)
Fe(OH)3(am)
(7)

Figure 1

Figure 2

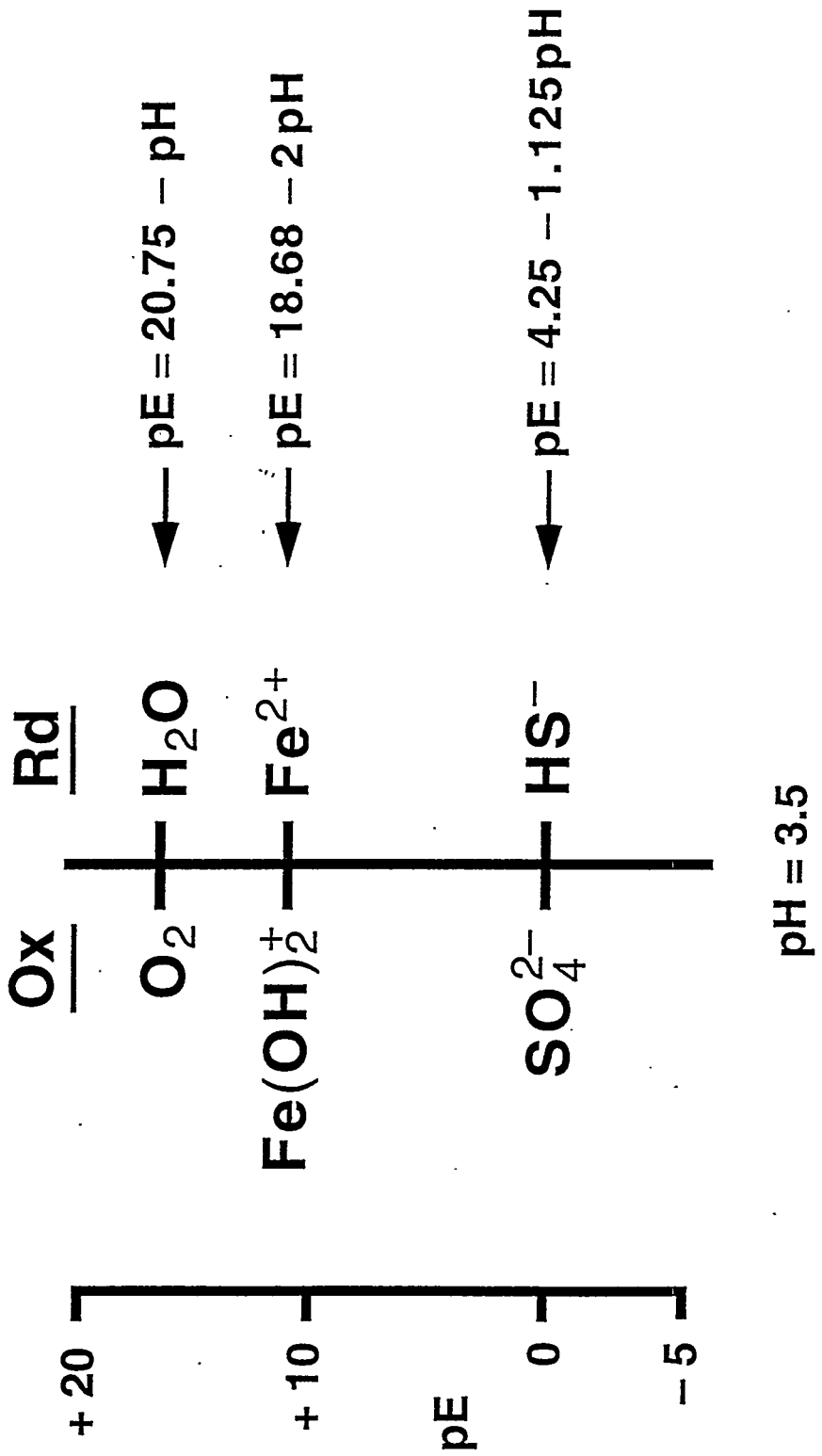
pE = 20.75 − pH
pE = 18.68 − 2pH
pE = 4.25 − 1.125pH
Rd
H2O
Fe2+
HS−
Ox
O2
Fe(OH)2+
SO4 2−
pH = 3.5
+ 20
+ 10
pE
0
− 5

Figure 3

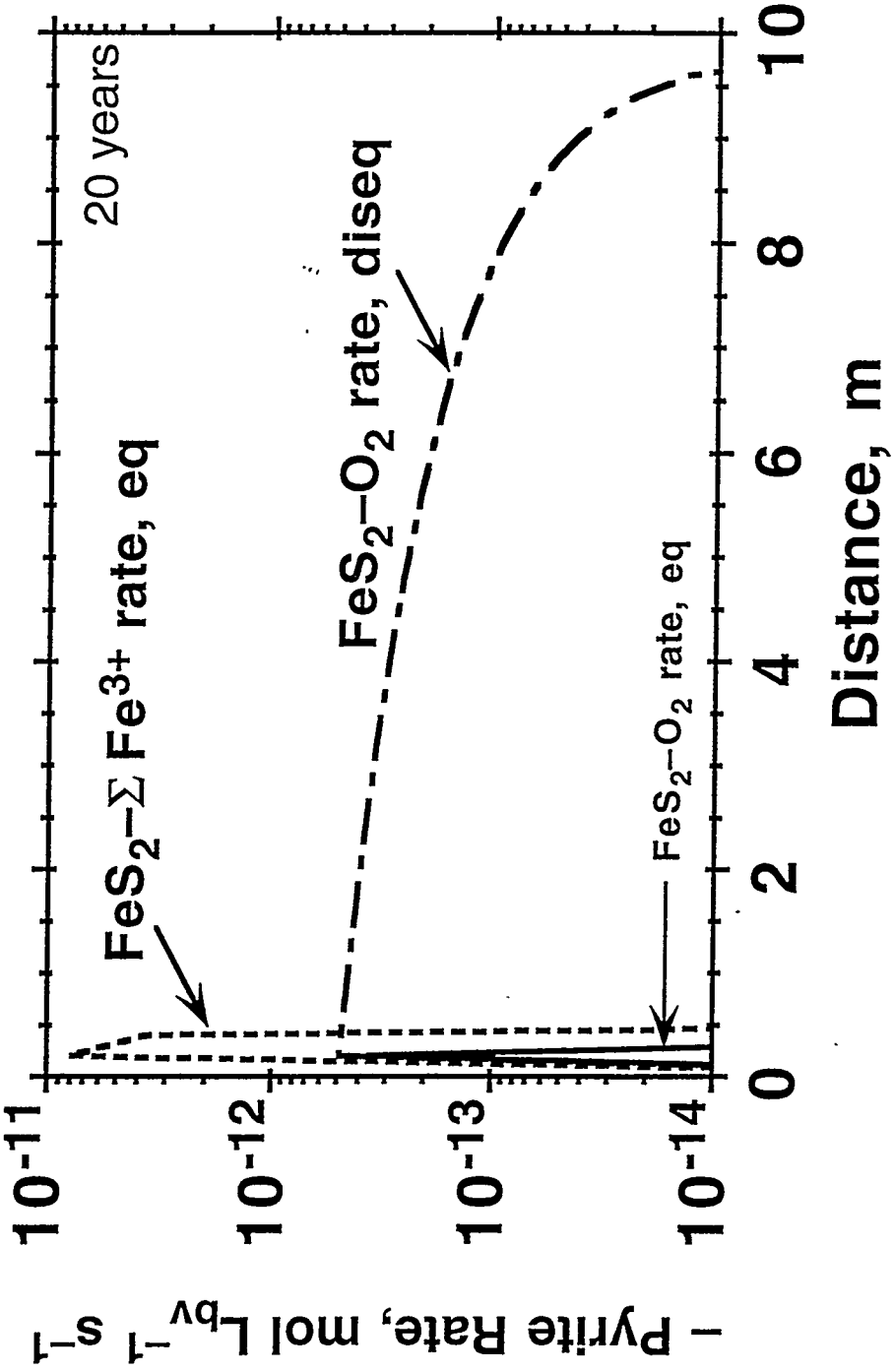
20 years
FeS_2–ΣFe^{3+} rate, eq
FeS_2–O_2 rate, diseq
FeS_2–O_2 rate, eq
– Pyrite Rate, mol L_{bv}^{-1} s^{-1}
10^{-11}
10^{-12}
10^{-13}
10^{-14}
0
2
4
6
8
10
Distance, m

Figure 4

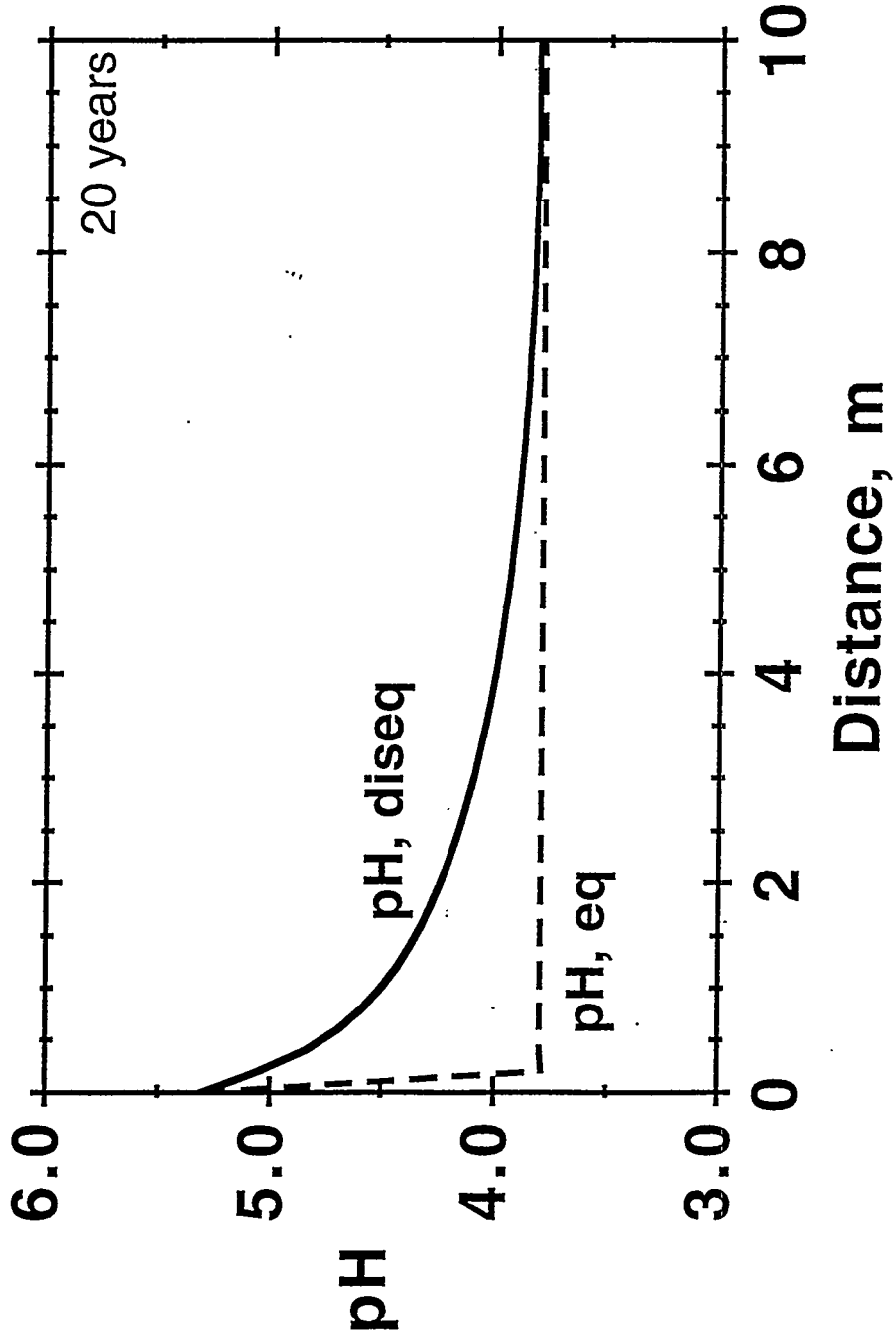

Figure 5

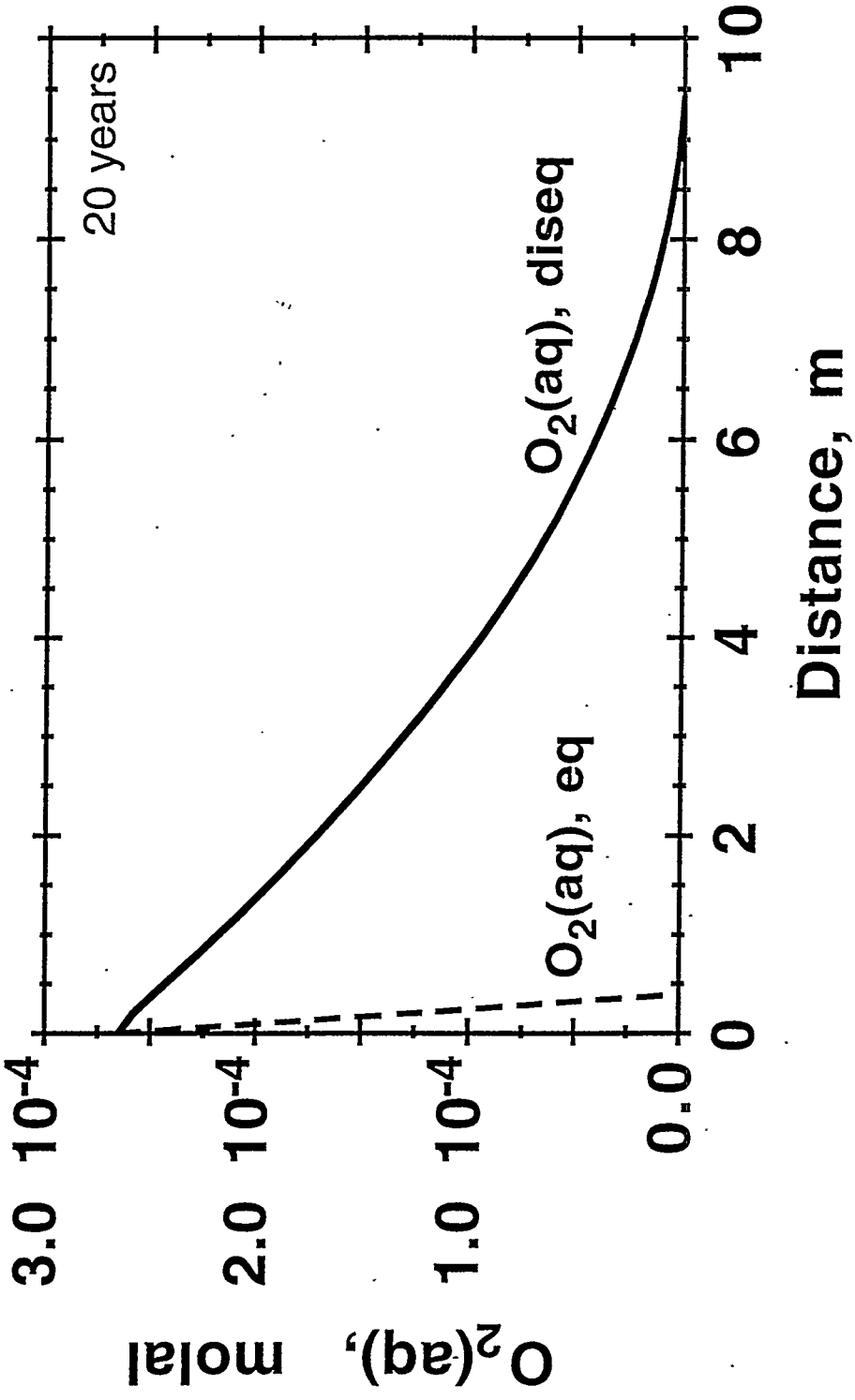
20 years
O_2(aq), diseq
O_2(aq), eq
O_2(aq), molal
3.0 10-4
2.0 10-4
1.0 10-4
0.0
0
2
4
6
8
10
Distance, m

Figure 6

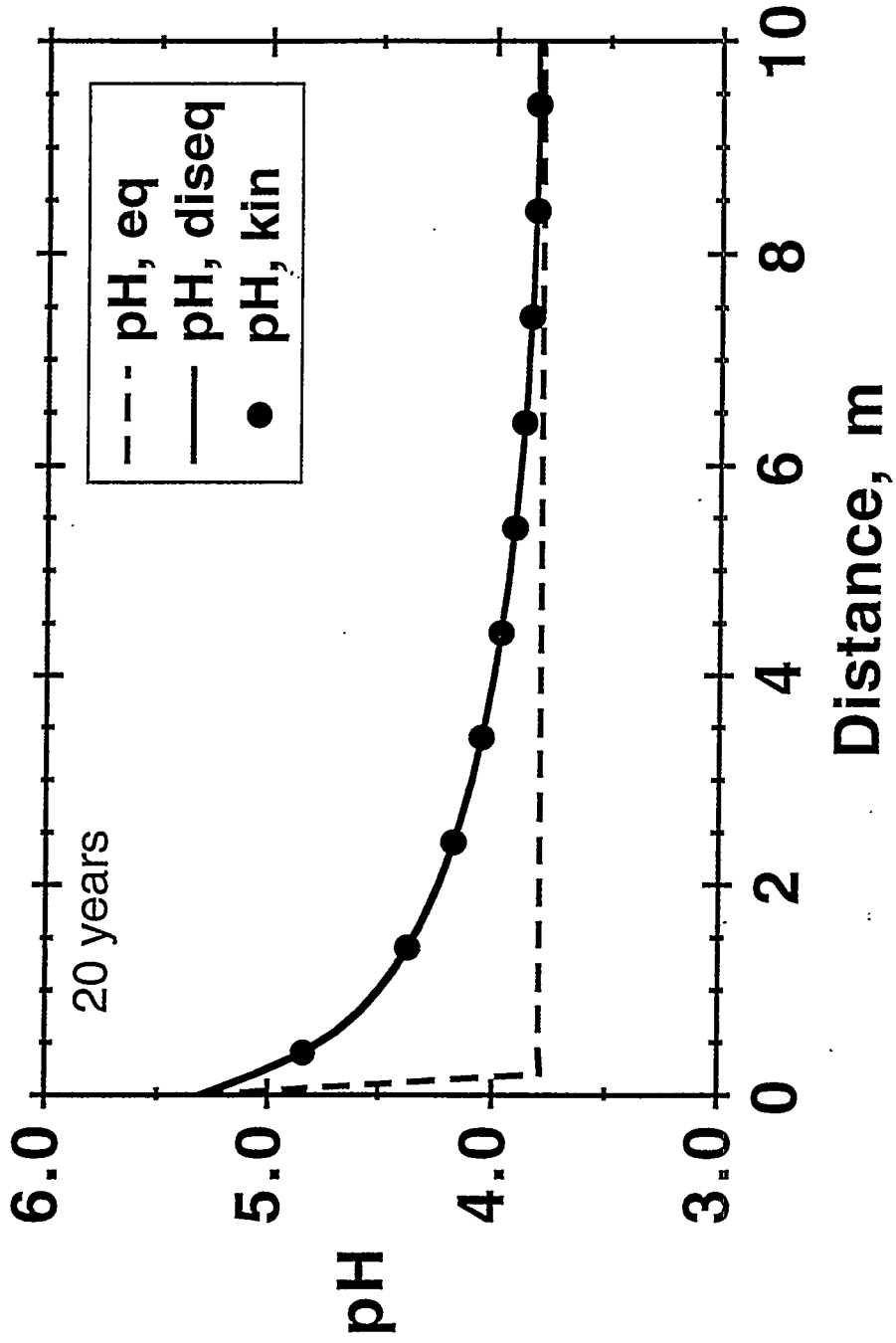

Figure 7

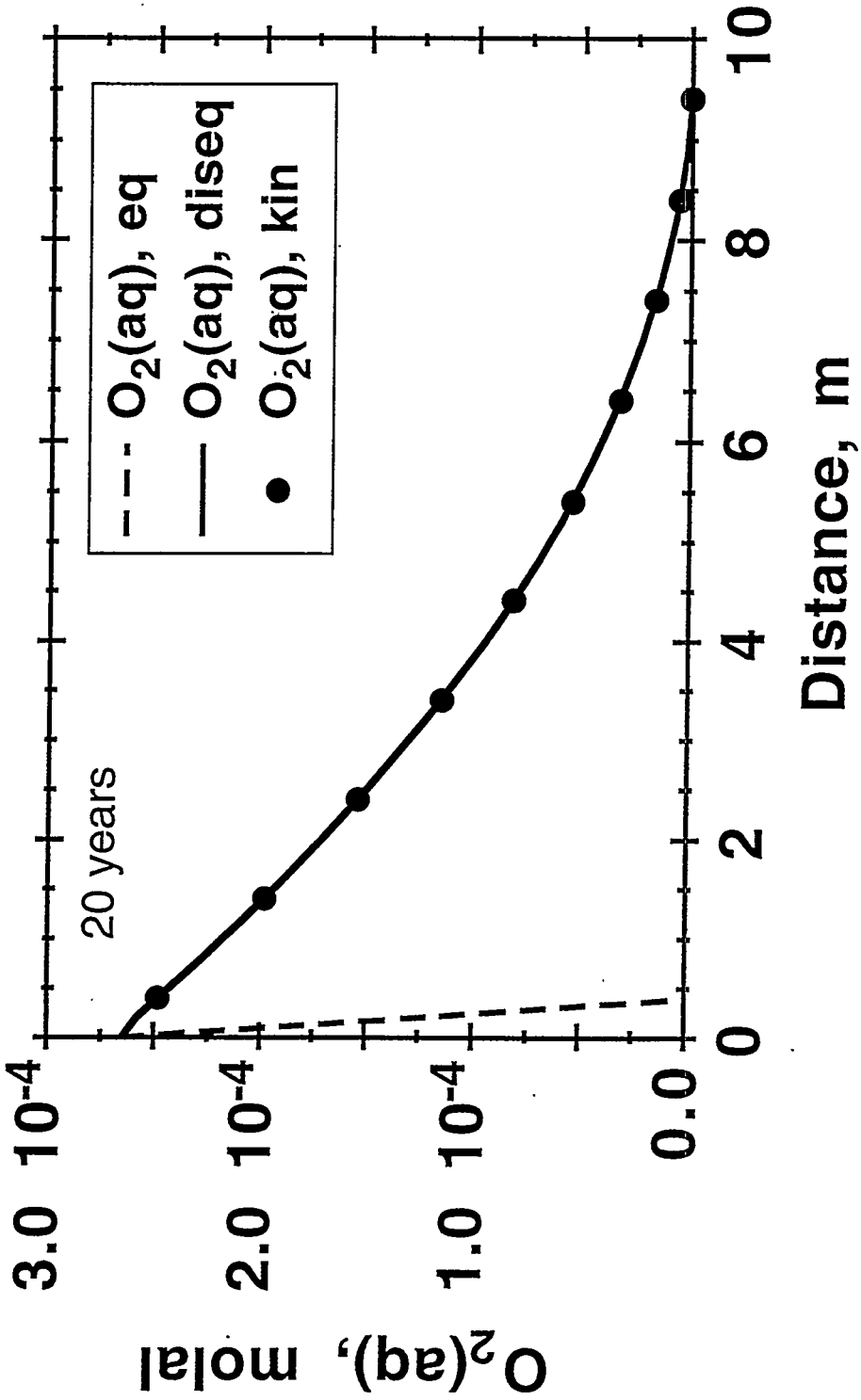
O_2(aq), eq
O_2(aq), diseq
O_2(aq), kin
20 years
O_2(aq), molal
3.0 10-4
2.0 10-4
1.0 10-4
0.0
0
2
4
6
8
10
Distance, m

Figure 8

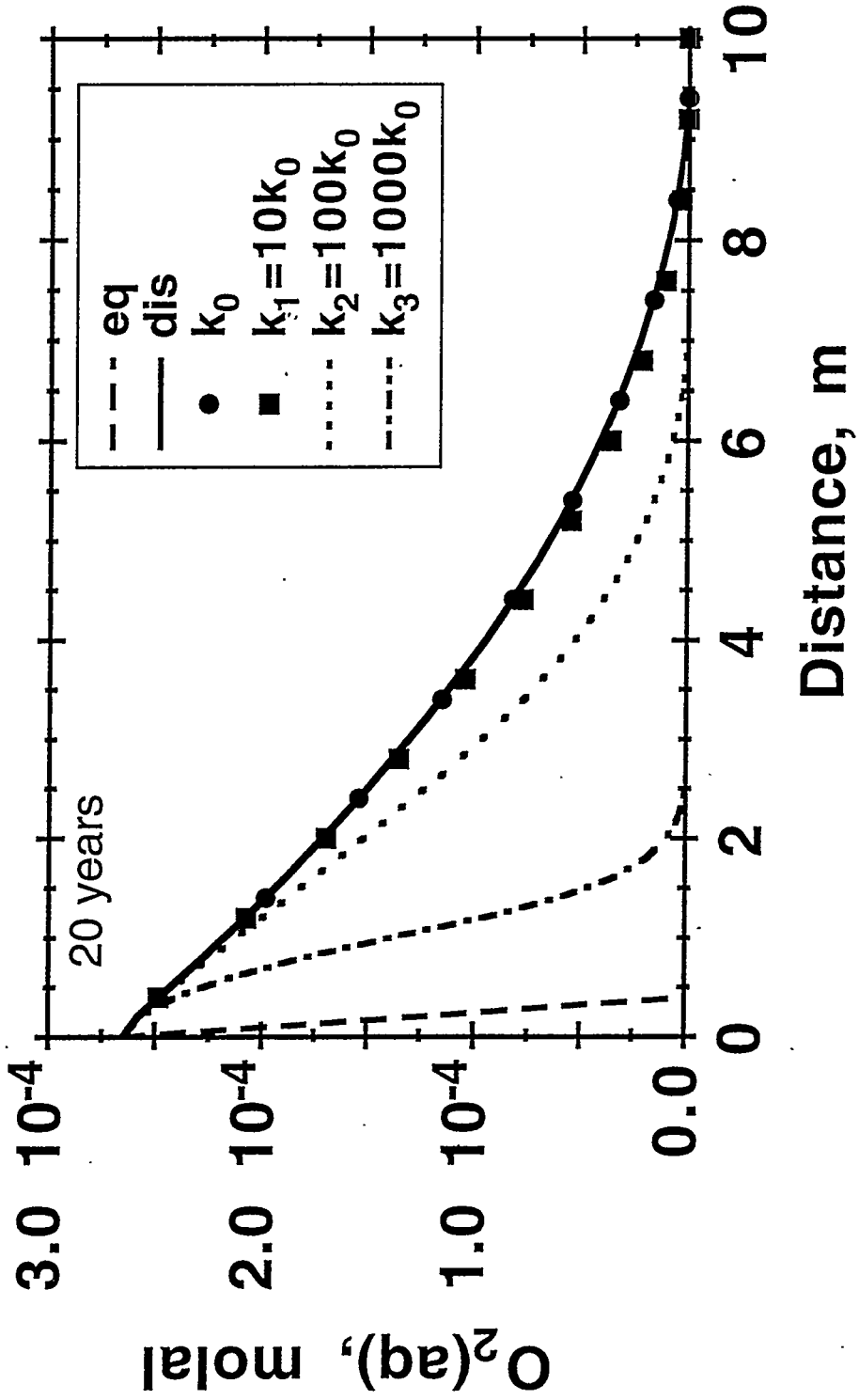
eq
dis
k_0
$k_1=10k_0$
$k_2=100k_0$
$k_3=1000k_0$
20 years
O_2(aq), molal
3.0 10^{-4}
2.0 10^{-4}
1.0 10^{-4}
0.0
0
2
4
6
8
10
Distance, m

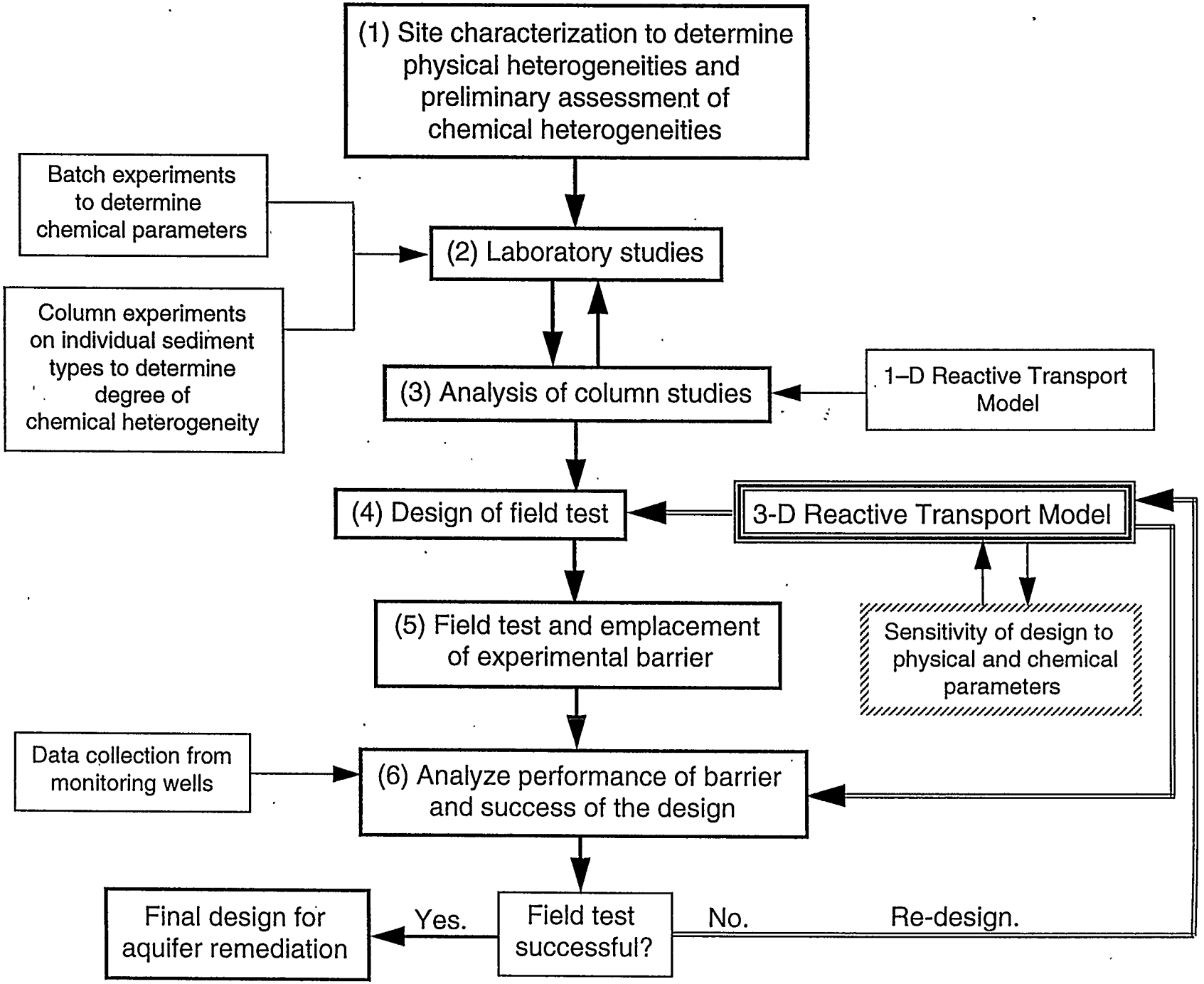
(1) Site characterization to determine physical heterogeneities and preliminary assessment of chemical heterogeneities
Batch experiments to determine chemical parameters
Column experiments on individual sediment types to determine degree of chemical heterogeneity
(2) Laboratory studies
(3) Analysis of column studies
1–D Reactive Transport Model
(4) Design of field test
3-D Reactive Transport Model
(5) Field test and emplacement of experimental barrier
Sensitivity of design to physical and chemical parameters
Data collection from monitoring wells
(6) Analyze performance of barrier and success of the design
Final design for aquifer remediation
Yes.
Field test successful?
No.
Re-design.

Figure 1

Table 1—Elements, minerals, and aqueous species used in pyrite oxidation simulations.

Figure 1—Pyrite oxidation model, showing the important reaction mechanisms (Stumm and Morgan, 1981).

Figure 2—Equilibrium redox ladder (Scott and Morgan, 1990).

Figure 3—Comparison of pyrite dissolution rates for intra-aqueous Fe equilibrium vs. intra-aqueous Fe disequilibrium. Both $O_2(aq)$ and Fe^{3+} induce significant dissolution in the equilibrium case, only $O_2(aq)$ is important in the disequilibrium case. (Here, the negative of the pyrite rate is plotted in units of moles per liter bulk volume per sec.)

Figure 4—Comparison of pH profiles for intra-aqueous Fe equilibrium vs. intra-aqueous Fe disequilibrium.

Figure 5—Comparison of $O_2(aq)$ concentration profiles for intra-aqueous Fe equilibrium vs. intra-aqueous Fe disequilibrium.

Figure 6—pH profile for intra-aqueous Fe kinetics (see Eq. 10) compared to intra-aqueous Fe equilibrium and intra-aqueous Fe disequilibrium.

Figure 7—$O_2(aq)$ concentration profile for intra-aqueous Fe kinetics (see Eq. 10) compared to intra-aqueous Fe equilibrium and intra-aqueous Fe disequilibrium.

Figure 8—pH profiles for various values of the Fe^{2+}–Fe^{3+} rate constant.

Figure 9—Flow chart of enhanced design methodology for *in situ* chemical barriers.